ISSN 0965-545X, Polymer Science, Series A, 2023, Vol. 65, No. 6, pp. 822–830. © Pleiades Publishing, Ltd., 2023.
ISSN 0965-545X, Polymer Science, Series A, 2023. © Pleiades Publishing, Ltd., 2023.

RHEOLOGY

Influence of Distribution Anisotropy and Particle Shape on Magnetorheological Properties of Magnetoactive Elastomers

S. A. Kostrov[a,b], V. S. Razakov[c], G. V. Stepanov[a,d], E. A. Olenich[b], V. V. Gorodov[b], and E. Yu. Kramarenko[a,*]

[a] *Faculty of Physics, Lomonosov Moscow State University, Moscow, 119991 Russia*

[b] *Enikolopov Institute of Synthetic Polymer Materials, Russian Academy of Sciences, Moscow, 117393 Russia*

[c] *MIREA Russian University of Technology, Lomonosov Institute of Fine Chemical Technologies, Moscow, 119571 Russia*

[d] *Research Institute of Chemistry and Technology of Organoelement Compounds, Russian Academy of Sciences, Moscow, 105118 Russia*

**e-mail: kram@polly.phys.msu.ru*

Received November 24, 2023; revised December 4, 2023; accepted December 8, 2023

Abstract—Viscoelastic properties of magnetoactive elastomers with spherical and plate-shaped filler have been studied. Four series of samples based on silicone elastomer and carbonyl iron microparticles have been prepared. A series of samples with a concentration of magnetic filler from 30 to 60 wt % which differed in the shape of filler particles (spherical and platelike) and in their distribution in the polymer matrix (isotropic and anisotropic). The magnetorheological properties of the obtained magnetoactive elastomers have been examined by dynamic mechanical analysis. Storage modulus values for samples of different compositions are in the range of 10–100 kPa. It has been shown that anisotropic materials are stiffer than the isotropic counterparts and demonstrate a higher magnetorheological effect: the increase in the elastic modulus of an anisotropic sample with the maximum filler content exceeds an order of magnitude in a magnetic field of 1 T. At the same filler concentrations, materials based on platelike iron are stiffer than those based on spherical iron. At low magnetic filler concentrations, the use of platelike iron makes it possible to achieve a higher magnetic response of the material; at high filler concentrations, the increase in the elastic modulus is greater for samples based on spherical particles. The anisotropic materials exhibit a more pronounced Payne effect.

DOI: 10.1134/S0965545X23600655

INTRODUCTION

Magnetoactive elastomers (MAEs) [1–7] represent a class of smart materials whose properties can be controlled using an external magnetic field. They consist of magnetic microparticles embedded in an elastic polymer matrix. When an external magnetic field is applied, the magnetic particles become magnetized. Due to dipole–dipole interactions and interaction with an external magnetic field, the particles tend to line up in chains along the lines of the external magnetic field [8–10]. Changes in the positions of magnetic particles and their interaction lead to changes in a wide range of physical properties of the material. For example, due to the fact that carbonyl iron, a typical magnetic filler, is a better conductor of electric current than the polymer matrix, the formation of chain-like structures leads to an increase in the conductivity and effective dielectric constant of the material in the direction of the chains. These phenomena are respectively called magnetoresistive and magnetodielectric effects [11–14]. In a magnetic field, particles tending to line up in chains can deform the surface of the material, changing its relief [15–17]; microstructuring of the filler also causes significant macroscopic strains of the samples: in a uniform magnetic field, uniaxial elongation of MAE is observed [18–20]. In this work, special attention is paid to the study of the viscoelastic properties of magnetic–polymer composites in a magnetic field, or the magnetorheological effect [4, 17, 21–23], which consists of an increase in the components of the dynamic modulus of MAE in an external magnetic field.

Magnetoactive elastomers are a relatively new materials whose the properties and magnetic response are determined by a wide range of parameters. In this work, the influence of the concentration of magnetic filler, the shape of magnetic particles, and their spacial distribution in the polydimethylsiloxane matrix were studied. The distribution anisotropy of the magnetic filler inside the polymer matrix can be set by perform-

ing MAE synthesis in an external magnetic field [24–38]. Oriented aggregates of magnetic particles, formed when a magnetic field is applied are fixed during the polymerization process, leading to changes in the properties of the material compared to isotropic counterparts [31, 39–41] and to the appearance of anisotropy in the properties of composites with oriented magnetic filler structures: for example, an anisotropic material can serve as a conductor, whereas an isotropic material is an insulator [24], the Young's modulus of an anisotropic material will depend on the sample stretching direction [30, 37]. In addition, magnetic particles arranged in chains will respond differently to an external magnetic field than particles uniformly distributed throughout the matrix due to their closer proximity to each other. Creating an anisotropic (chain-like) profile of the distribution of magnetic particles is one of the main ways to program the movement of soft magnetic polymer robots [26–29].

The properties of MAEs based on anisometric magnetic particles have barely been studied. In a theoretical work [42], it was shown that the rotation of magnetic particles under the action of an external magnetic field significantly affects the MAE surface relief. Also recently, the influence of distribution anisotropy and shape of magnetic filler particles on the mechanical properties of magnetic polymer composites in the absence of a magnetic field has been studied experimentally [43]. It was found that the anisotropy of mechanical properties is most pronounced in MAE based on anisometric particles, namely, needle-like magnetite and platelike iron.

In this work, we synthesized MAEs based on PDMS and carbonyl iron with platelike and spherical shapes. Two series of samples with an isotropic and anisotropic distribution of magnetic particles with concentration from 30 to 60 wt % were created on the basis of both types of magnetic filler. Reducing the elastic modulus of the polymer matrix is an important task to achive a high magnetic response of the material, since a rigid medium prevents the displacement of magnetic particles inside the material. A feature of the polymer matrix used in this work is the presence of side chains at the network nodes. Side chains are not elastically active, but they increase the total volume of the system, thereby reducing the elastic modulus of the material by decreasing the crosslink density [44]. This approach eliminates the use of low-molecular-weight oil and enhances system stability because the side chains do not bleed out of the sample as oil does, since they are chemically bonded to the polymer matrix.

MATERIALS

The following reagents and auxiliary agents were used in the study: 1,1,3,3,5,5-hexamethylcyclotrisiloxane (D_3) (97%), 1,1,3,3,5,5,7,7-octamethylcyclotetrasiloxane (D_4) (98%) (both from ABCR), 1,1,3,3-tetramethyldisiloxane (Sigma Aldrich), CT 175 sulfonic cation-exchange resin (Purolite), 7% hexachloroplatinic acid solution in isopropyl alcohol (Speier's catalyst) (Sigma Aldrich), vinyldimethylchlorosilane (ABCR), 2.7 M *n*-butyllithium solution in toluene (Acros), hexane of the reagent grade (Rushim.ru), analytical grade tetrahydrofuran (Ruskhim.ru), analytical grade toluene (Khimpromtorg), α,ω-divinylpolydimethylsiloxane of the DVK-5 brand (Penta-91), polymethylhydrosiloxane P-804 (Penta-91), spherical carbonyl iron R-20

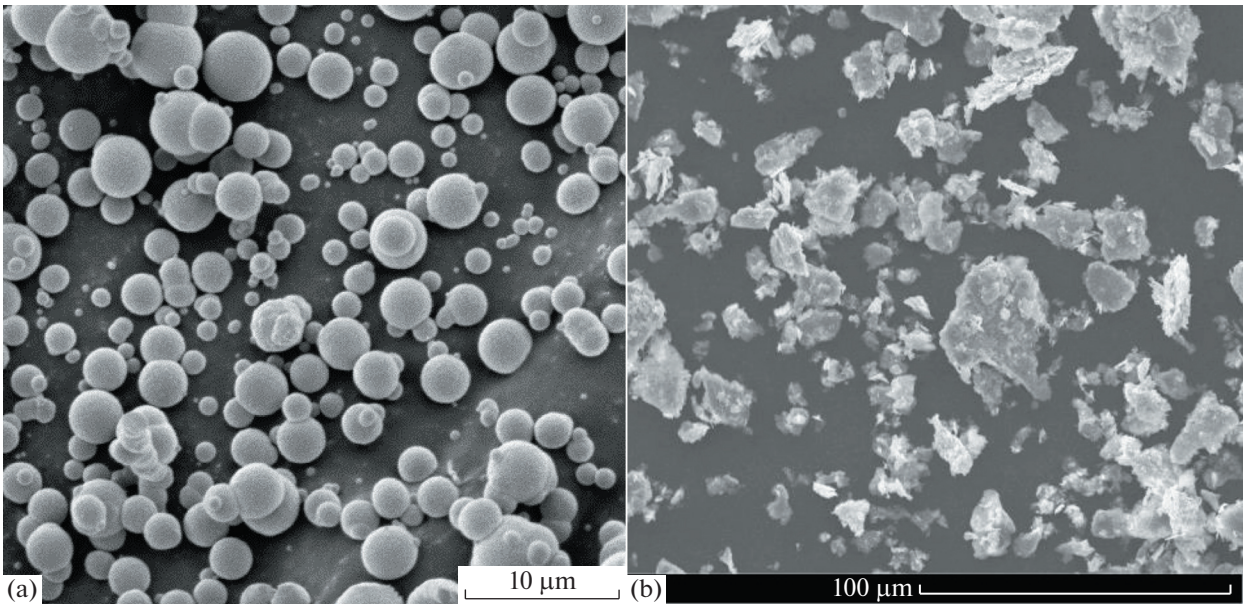

Fig. 1. Micrographs of (a) spherical and (b) platelike magnetic particles of carbonyl iron. Color drawings can be viewed in an electronic version.

(Spektr-Khim) of 3–5 μm in diameter, and plate-shaped iron with an average size of 20 μm obtained by grinding carbonyl iron in a planetary mill [43]. Scanning electron microscope images of magnetic particles are presented in Fig. 1. Toluene and THF were dried over metallic sodium and distilled, and the other aforementioned substances were used without further purification.

SYNTHESIS

Bifunctional PDMS

Cationic polymerization. Preparation of telechelic hydride-containing PDMS. 1,1,3,3,5,5,7,7-Octamethylcyclotetrasiloxane (D_4) in an amount of 50 g (0.1689 mol) and 11.32 g (0.0845 mol) of 1,1,3,3-tetramethyldisiloxane were placed into a one-necked flask equipped with a reflux condenser and a drying tube, and then 1.84 g of Purolite CT-175 sulfonic acid cation-exchange resin was added. The mixture was stirred in the block for about 15–18 h at a temperature of 70°C. Then the resulting mixture was dissolved in hexane and filtered through filter paper to remove the residual cation-exchange resin. The filtrate was evaporated on a rotary evaporator. To remove cyclic compounds, the product was reprecipitated from toluene into ethanol and the remaining low-molecular-weight substances were distilled off at 1 mmHg at a temperature of 130°C to constant weight. We obtained 52.12 g of desired product. The reaction yield is 85%. ^{1}H NMR ($CDCl_3$): δ_H = 0.08 ppm (s, $Si(CH_3)_2$), 4.71 ppm (t, SiH). GPC: $M_n = 1.7 \times 10^3$, $M_w = 2.3 \times 10^3$, $M_w/M_n = 1.38$.

Monofunctional PDMS

Anionic polymerization. Preparation of monofunctional PDMS. In a one-necked flask equipped with a magnetic stirrer and a reflux condenser and placed in an inert environment, 100 g (0.4495 mol) of hexamethylcyclotrisiloxane (D_3), 250 mL of toluene, 27 mL of a 2.7 M of *n*-butyllithium solution in toluene were loaded; the mixture was stirred for 10 h; and 150 mL of THF was added. The mixture was stirred for 6 h, and then 19 mL (0.138 mol) of vinyldimethylchlorosilane was added followed by stirring for 10 h. The resulting mixture was filtered through filter paper, the filtrate was evaporated on a rotary evaporator, and low-molecular-weight reaction products were distilled off at 1 mmHg at a temperature of 130°C. The yield was 90 g or 85%. ^{1}H NMR ($CDCl_3$): δ_H = 6.19–5.67 ppm (m, 3H, Si–CH=CH_2), 1.34–1.26 ppm (m, 5H, $\underline{CH_3}$–$\underline{CH_2}$–CH_2–CH_2–$(Si(CH_3)_2O)_n$–$Si(CH_3)_2$–H), 0.89 ppm (t, 2H, CH_3–$\underline{CH_2}$–CH_2–CH_2– $(Si(CH_3)_2O)_n$–$Si(CH_3)_2$–H), 0.54 ppm (m, 2 H CH_3–CH_2–CH_2–$\underline{CH_2}$–$(Si(CH_3)_2O)_n$–$Si(CH_3)_2$–H), 0.08 ppm (s, CH_3–CH_2–CH_2–CH_2–$\underline{(Si(CH_3)_2O)_n}$–$Si(CH_3)_2$–H). GPC: $M_n = 4.7 \times 10^3$, $M_w = 5.2 \times 10^3$, $M_w/M_n = 1.10$.

Below is a reaction scheme for the preparation of telechelic hydride-containing PDMS (a), the final reaction product (b), as well as a scheme for the preparation of monofunctional vinyl-containing PDMS (c) and the final reaction product (d).

(a)

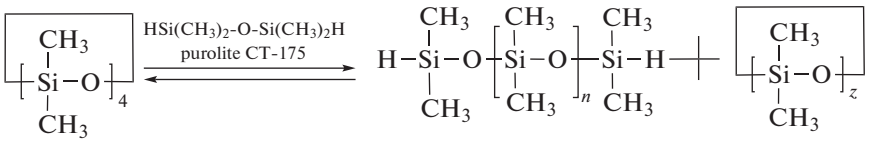

(b)

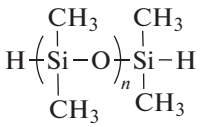

(c)

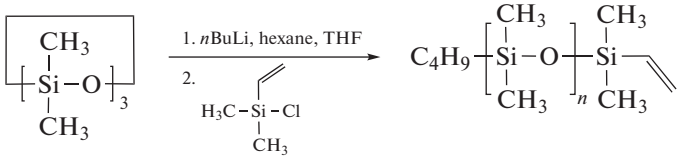

(d)

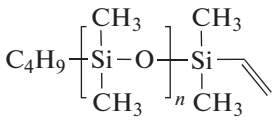

Scheme 1.

Polymer Matrix

The following four components were used in the compositions to obtain the matrices: 5 g of α,ω-divinyl-polydimethylsiloxane Vinyl Silicone Oil 5000 cSt as a base rubber, 0.0486 g of polymethylhydride siloxane P-804 as a crosslinking agent; 1.6981 g of ω-vinyl-oligodimethylsiloxane as side chains grafted to the crosslinker; and 0.1621 g of α,ω-dihydride-oligodimethylsiloxane as an extender of the base rubber. The synthesis of the polymer matrix was described in detail in our previous paper [17]. The role of the side chains is to reduce the functionality of the crosslinker and dilute the system without increasing the number of elastically active segments. After mixing all the polymer components, carbonyl iron was added to the mixture. Speier's catalyst was used as a catalyst, which was introduced into the system at this step in a ratio of 10 μL of a solution in isopropanol per 1 g of mixture. After thorough mechanical mixing, the mixture was degassed at a pressure of ~1 mm Hg to remove air bubbles trapped the mixture during stirring. The curing mixture was then poured into a closed mold of the required thickness, which was placed into an owen at a temperature of 90°C for vulcanization. To set the anisotropic distribution of magnetic particles, a pair of permanent magnets of 50 mm in a diameter with a magnetic field of ~0.34 T near the surface was applied to the mold on both sides during vulcanization. After curing, the films were removed from the mold and disks with a diameter of 20 mm and a thickness of ~1 mm were cut out for the subsequent measurement of magnetorheological properties. As a result, four series of MAE were obtained with a magnetic filler concentration from 30 to 60 wt % based on platelike and spherical carbonyl iron with isotropic and anisotropic distributions. It is noteworthy that achieving a higher concentration of platelike iron is a difficult task. Platelike particles have a high specific surface area, due to which they adsorb the polymer and thicken the composition, bringing it to the consistency of a paste, from which it is difficult to mold the elastomer of the required size.

INVESTIGATION TECHNIQUES

GPC analysis was carried out using a chromatographic system consisting of a Shimadzu LC-20AT high-pressure pump, a Knauer Smartline RI 2300 refractometer, and a Knauer Jetstream 2 Plus thermostat at a temperature 40°C (±0.1°C) with toluene–2% THF as the eluent pumped at a flow rate of 1.0 mL/min. Columns of a 300 × 7.8 mm size were packed with Phenogel (Phenomenex, USA) having a particle size of 5 μm and pores from 10^3 to 10^5 Å. The columns were calibrated using Agilent polystyrene standards. Processing of chromatograms and calculation of molecular weight parameters were performed using the MultiChrome program for Windows, version 1.6 (GPC) (Ampersend, Russia).

^{1}H NMR spectra were recorded with a Bruker WP-250 SY spectrometer using $CDCl_3$ as the solvent and the ACD/Labs software for spectra viewing and processing.

The viscoelastic properties of MAEs were measured using an Anton Paar Physica MCR 302 rheometer with a plate–plate measuring system and an MRD 170/1 T magnetic cell equipped with an electromagnet. The MAE sample was placed between the measuring head and the substrate plane. Shear oscillations were applied to the sample being measured, during which the strain of the sample changed according to the harmonic law $\gamma = \gamma_0\sin(\omega t)$, where γ is the shear strain, γ_0 is the strain amplitude, and ω is the oscillation frequency. The response of the sample to strain was measured: shear storage modulus G' and loss modulus G'', which are responsible for the elastic and viscous response of the sample, respectively. The damping factor $\tan\delta = G''/G'$ was also calculated, which characterizes the proportion of energy loss during one load cycle of the material. Experiments were carried out at room temperature. The normal force in all experiments was approximately $F_N \sim 1$ N. Frequency dependences were measured at a fixed oscillation amplitude $\gamma_0 = 0.1\%$ in the frequency range of $\omega = 1$–100 rad/s, and amplitude dependences were measured at a fixed oscillation frequency of $\omega = 10$ rad/s in the amplitude range of $\gamma_0 = 0.02$–20%. The dependences of the components of the dynamic modulus of the samples on the magnetic field strength were obtained in the linear viscoelasticity mode at a fixed oscillation amplitude $\gamma_0 = 0.1\%$ and an oscillation frequency of $\omega = 10$ rad/s. The magnetic field was applied perpendicular to the sample plane; i.e., in experiments with anisotropic samples, the direction of the external magnetic field coincided with the orientation direction of magnetic filler chains.

RESULTS

Frequency Dependences

Figure 2 shows the dependences of the storage modulus of MAE samples with carbonyl iron concentrations of 60 and 40 wt % based on platelike and spherical magnetic particles, as well as with isotropic and anisotropic distribution of magnetic filler in the absence of a magnetic field and in a magnetic field of $B = 1$ T. Here and below, the curves with red circles and blue squares refer to samples based on the spherical and platelike filler, respectively. The dashed lines refer to the anisotropic materials, and the open symbols refer to measurements made in a magnetic field of

$B = 1$ T. Figure 3a shows that the storage modulus of the materials increases several times when a magnetic field is applied. For an anisotropic sample containing 60 wt % spherical magnetic particles, the relative increase in the elastic modulus exceeds an order of magnitude (Fig. 3a), which is significant for MAE with a rather low degree of filling. Higher MAE response values with initial storage moduli of ~10–30 kPa are achieved by increasing the filler content to 80–83 wt % [10, 17, 31, 45]; however, as noted above, it is difficult to achieve a concentration of magnetic particles above 60 wt % because of the strong thickening of the vulcanization mixture in the case of using platelike particles with a large specific surface area. Since the goal of the study was a comparative analysis of the properties of MAEs based on particles of different shapes, the concentration of spherical particles in the samples was limited to the highest attainable one for the MAE based on platelike particles. Figure 3 shows that the thickening of the system by changing the particle shape also plays a role after vulcanization: samples based on platelike magnetic particles have higher storage moduli than those based on spherical particles, both for the isotropic and anisotropic materials (see also Tables 1 and 2), which is more pronounced for highly filled samples. This conclusion is consistent with the result reported in [43]. Anisotropic magnetic compositions have a two to three times higher storage modulus than the isotropic ones in agreement with published data [25, 32–34, 36, 38]. At lower concentrations of magnetic filler (Fig. 3b), the storage modulus in a magnetic field for MAE samples based on platelike particles turns out to be higher than that of both isotropic and anisotropic samples of MAE based on spherical particles.

To analyze the influence of the particle shape on the properties of MAEs at different fillings, the dependences of the initial storage modulus, the storage modulus in a magnetic field of $B = 1$ T, and the relative growth in the storage modulus in a magnetic field of $B = 1$ T for all obtained MAEs on the concentration of magnetic particles were plotted (Fig. 3). From the presented dependences it is clear that an increase in the filler concentration leads to an increase in the storage modulus of all samples both in the absence of magnetic field and in a field of 1 T. Anisotropic samples are two to three times stiffer than the isotropic ones, and samples based on platelike iron are stiffer than those based on spherical iron over the entire concentration range. As for the influence of particle shape on the magnetic response, it manifests itself differently at low and higher filler contents. At low concentrations of magnetic filler, the MAE storage modulus G'_{max} and its relative increase in a magnetic field are greater for samples based on platelike iron than those based on spherical iron. At magnetic filler concentrations of $\varphi_{Fe} > 45$ wt %, the samples based on spherical iron begin to demonstrate a higher magnetorheological effect. This is presumably due to the fact that at low filler concentrations, a significant contribution to the change in the internal structure of the material based on platelike particles is made by their rotations in a magnetic field—being directed parallel to the plane of the particles, the magnetic moment of the particles tends to turn along the magnetic field lines. As the concentration increases, the rotation and movement of platelike particles in an applied magnetic field becomes difficult due to steric restrictions. This occurs at lower concentrations than for spherical particles, since the percolation threshold decreases and particle interactions increase in the case of high anisometry. As a result, the magnetic response of MAEs based on anisometric platelike particles becomes smaller than that of MAEs based on the spherical filler. The values of the measured magnetorheological characteristics of all obtained MAEs are presented in Tables 1 and 2.

Table 1. Magnetorheological characteristics of MAE samples based on spherical carbonyl iron at an angular frequency of oscillations $\omega = 10$ rad/s and a small strain amplitude of $\gamma = 0.1\%$

φ_{Fe}, wt %	G'_0, kPa		tanδ		G'_{max}, kPa		G'_{max}/G'_0	
	iso	aniso	iso	aniso	iso	aniso	iso	aniso
30	8.6	12.9	0.11	0.16	13.2	32.8	1.5	2.5
40	10.5	21.6	0.17	0.17	22.9	85.6	2.2	4.0
45	11.8	45.4	0.11	0.126	21.5	148	1.8	3.3
50	16.6	35.2	0.15	0.11	57.8	94.3	3.5	2.7
60	15.9	54.3	0.2	0.2	87.3	668	5.5	12.3

Amplitude Dependences

Filled elastomers are characterized by the so-called Payne effect [46–48], which consists in a decrease in the storage modulus of the material with increasing strain amplitude. Strain softening of the composite material is explained by the destruction of aggregates of filler particles and a decrease in the force of their interaction with increasing distance between them under mechanical action. In the limit of high strains, the storage modulus of the composite tends to the storage modulus of the polymer matrix [47]. This effect is even more pronounced for magnetic elastomers, since magnetic particles interact with each other through long-range magnetic forces. Figure 4 shows

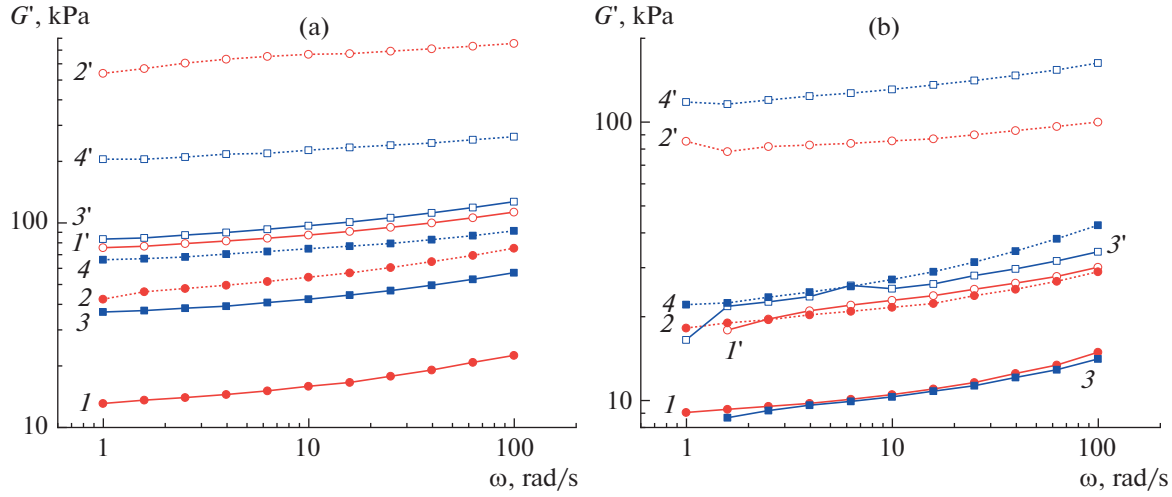

Fig. 2. Dependences of the storage modulus on the angular frequency of shear strain of MAE samples with a magnetic filler concentration of (a) 60 and (b) 40 wt % and based on (*1*, *1*', *2*, *2*') spherical and (*3*, *3*', *4*, *4*') platelike carbonyl iron with (*1*, *1*', *3*, *3*') isotropic and (*2*, *2*', *4*, *4*') anisotropic distribution of magnetic particles ((*1*–*4*) in the absence of a magnetic field and (*1*'–*4*') in a magnetic field of magnitude $B = 1$ T). Carbonyl iron concentration, 60 wt %. Frequency dependences for samples with other concentrations of magnetic filler are given in the Supplementary Materials (Fig. S1).

the dependence of the storage modulus of the samples on the amplitude of shear oscillations for MAEs, based on platelike and spherical magnetic particles, with a carbonyl iron concentration of 60 wt % and in the cases of isotropic and anisotropic distribution of the magnetic filler in the absence of magnetic field and in a magnetic field of $B = 1$ T. It can be seen that the decrease in the storage modulus is more pronounced for anisotropic samples; this is due to the fact that their initial storage modulus is higher at low strains and the storage modulus of the composite at high strains tends to the storage modulus of the polymer. This result is consistent with the published data [31, 49]. This feature is characteristic of all obtained MAE samples (Supplementary Materials, Fig. 2S).

Table 2. Magnetorheological characteristics of MAE samples based on platelike carbonyl iron at an angular frequency of oscillations $\omega = 10$ rad/s and a small strain amplitude of $\gamma = 0.1\%$

φ_{Fe}, wt %	G'_0, kPa		tanδ		G'_{max}, kPa		G'_{max}/G'_0	
	iso	aniso	iso	aniso	iso	aniso	iso	aniso
30	6.4	17.1	0.28	0.28	15	76.1	2.3	4.5
40	10.3	27.2	0.15	0.27	25.2	131	2.4	4.8
45	15.7	46.9	0.20	0.17	51.1	111	3.3	2.4
50	27.6	58.5	0.13	0.16	75	161	2.7	2.8
60	42.4	74.8	0.17	0.16	97	227	2.3	3.0

Magnetic Field Dependences of Viscoelastic Properties of MAEs

Figure 5 shows the magnetic field dependences of the real and imaginary parts of the dynamic modulus of elasticity obtained for MAE with a carbonyl iron concentration of 60 and 40 wt % based on platelike and spherical magnetic particles, as well as with an isotropic and anisotropic distribution of the magnetic filler. Hysteresis of MAE properties in a magnetic field is a characteristic property of magnetic–polymer composites. This effect is due to the combination of elastic and magnetic properties in the composite material. Moreover, carbonyl iron itself is a soft magnetic material. The position of magnetic particles inside the material is determined by the balance of elastic forces of the polymer matrix, which tend to keep the particles in their initial position, and magnetic forces, which are stronger the closer the particles are to each other. Consequently, particles that have come closer together as the magnetic field increases are more difficult to separate when the curve "reverses." It is worth noting that depending on the magnetic filler content, the effectiveness of magnetic particles of various shapes in forming the magnetic response of the material changes. At low fillings, platelike particles strengthen the material more strongly than spherical ones over the entire range of magnetic field variations, since they are magnetized along the plane of the particles, rotate with edges along the external field, and form a percolation cluster at lower concentrations.

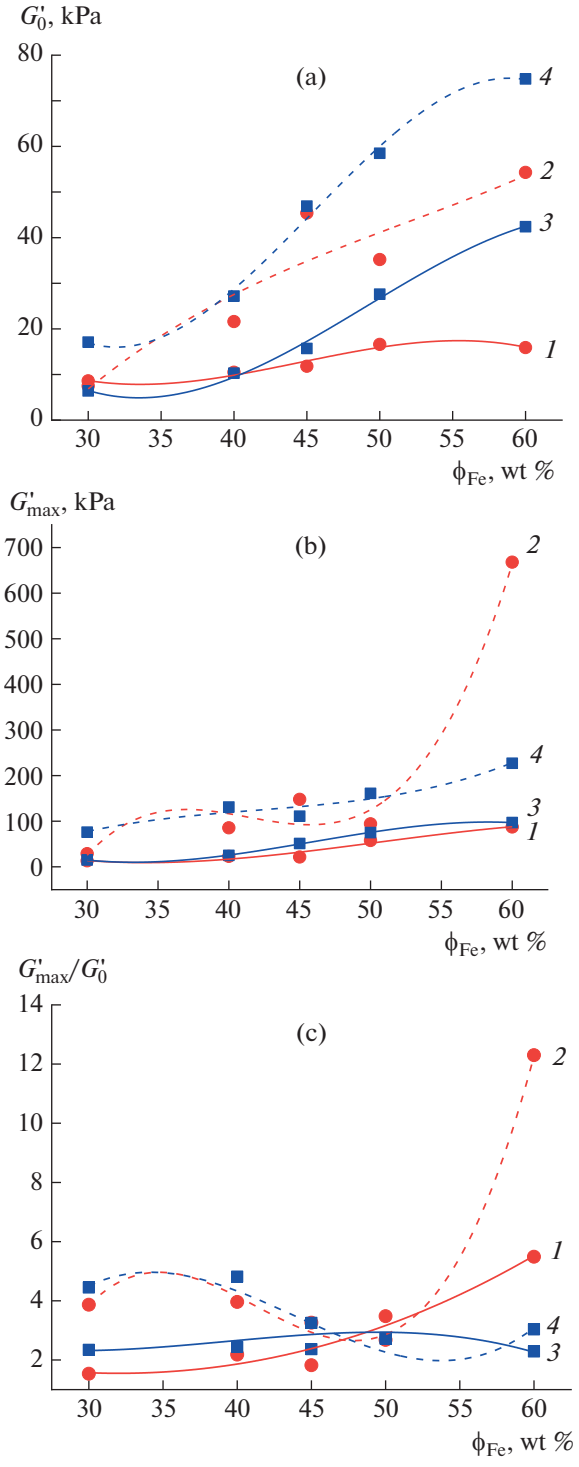

Fig. 3. Dependences on the mass concentration of iron particles for (a) the storage modulus in the absence of magnetic field, (b) the storage modulus in a magnetic field of $B = 1$ T, and (c) the relative increase of the storage modulus in a magnetic field of $B = 1$ T for MAEs based on (*1*, *2*) spherical and (*3*, *4*) platelike carbonyl iron with (*1*, *3*) isotropic and (*2*, *4*) anisotropic distribution of magnetic filler. The characteristics are given at an angular oscillation frequency of $\omega = 10$ rad/s and a small strain amplitude of $\gamma = 0.1\%$.

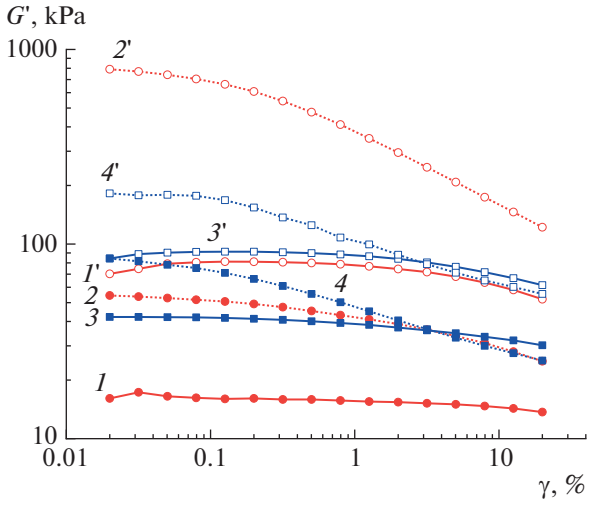

Fig. 4. Dependence of the storage modulus on the shear strain amplitude for MAEs based on (*1*, *1*', *2*, *2*') spherical and (*3*, *3*', *4*, *4*') platelike carbonyl iron with (*1*, *1*', *3*, *3*') isotropic and (*2*, *2*', *4*, *4*') anisotropic distribution of magnetic particles (*1*–*4*) in the absence of a magnetic field and (*1*'–*4*') in a magnetic field of $B = 1$ T. The concentration of carbonyl iron is 60 wt %. Amplitude dependences for samples with other concentrations of magnetic filler are given in the Supplementary Materials (Fig. S2).

CONCLUSIONS

Magnetic–polymer compositions based on cross-linked PDMS with comb-shaped segments and magnetic particles of platelike and spherical carbonyl iron have been obtained. A comparative analysis of the viscoelastic properties and magnetic response of isotropic and anisotropic (synthesized in an external magnetic field) samples with a magnetic filler concentration of 30 to 60 wt % in magnetic fields of up to 1 T was carried out.

It has been shown that the values of the storage modulus of the obtained materials lie in the range of 10–100 kPa. The storage modulus increases with increasing concentration of the magnetic filler, whereas composites based on platelike particles turn out to be stiffer than those based on spherical ones, a difference that is explained by the large specific surface area of anisometric particles. The distribution anisotropy of the magnetic filler also leads to strengthening of the material in the direction of orientation of chainlike aggregates of magnetic particles, which is consistent with published data.

At low concentrations of magnetic filler, the relative growth of the storage modulus in a magnetic field of 1 T is higher for materials based on platelike iron, which are aligned with the plate edges along the field, forming a percolation cluster. At filler concentrations greater than 45 wt %, the use of spherical iron particles is more effective in obtaining a material with a high magnetic response. The maximum relative growth of the storage modulus in a magnetic field is achieved for

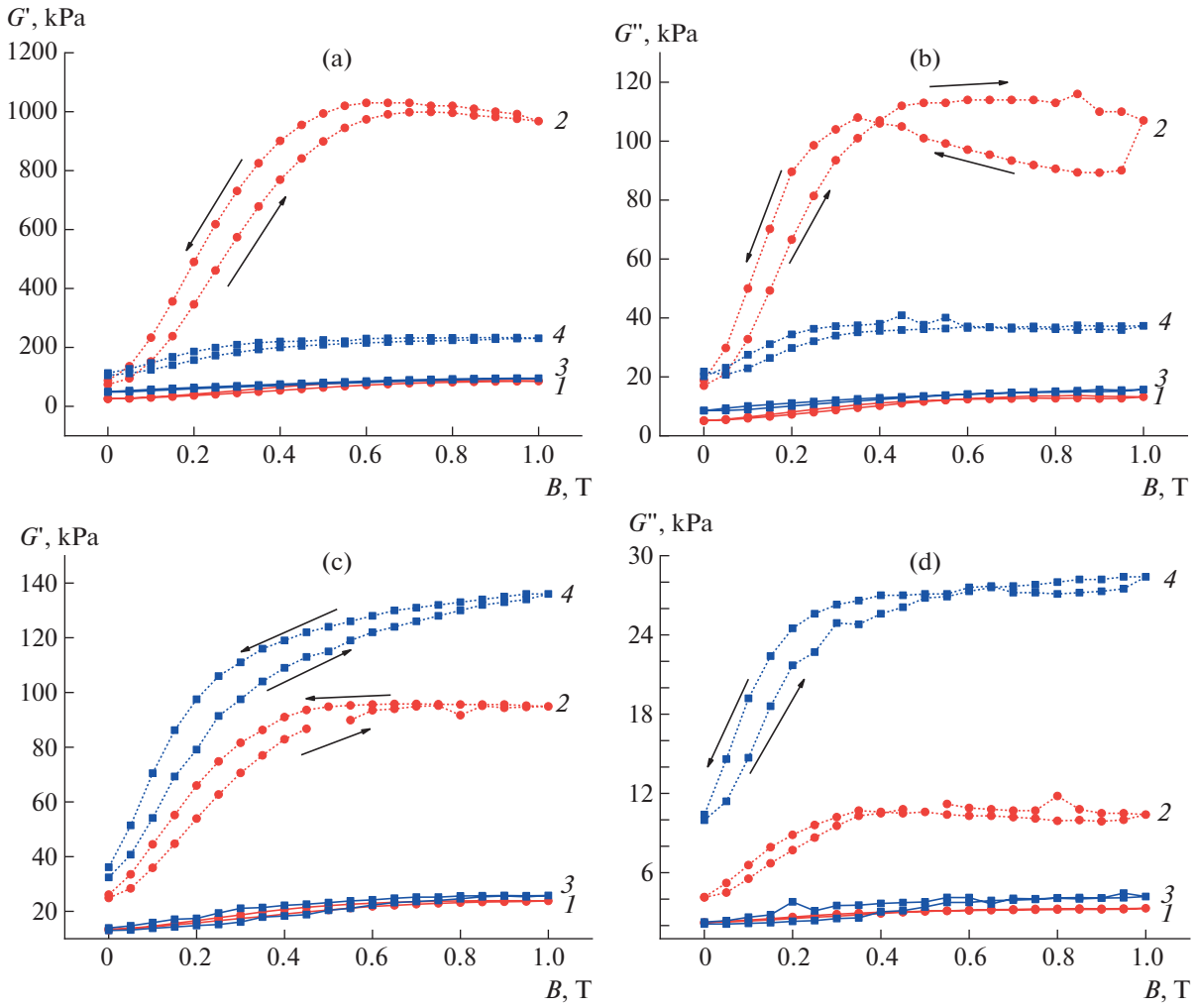

Fig. 5. Magnetic-field dependences of the (a, c) real and (b, d) imaginary components of the dynamic elastic modulus of MAEs based on (*1*, *2*) spherical and (*3*, *4*) platelike carbonyl iron with (*1*, *3*) isotropic and (*2*, *4*) anisotropic distribution of magnetic filler. The concentration of carbonyl iron is (a, b) 60 and (c, d) 40 wt %. Field dependences for samples with other concentrations of magnetic filler are given in the Supplementary Materials (Fig. S3).

an anisotropic sample based on spherical particles (60 wt %) and exceeds one order of magnitude.

The Payne effect, which consists in a decrease in the elastic modulus of the composite with increasing strain amplitude, is less pronounced for samples with an isotropic distribution of the magnetic filler.

SUPPLEMENTARY INFORMATION

The online version contains supplementary material available at https://doi.org/10.1134/S0965545X23600655

FUNDING

NMR and GPC studies were carried out at the Shared-Use Center "Polymer Research Center" of the Enikolopov Institute of Synthetic Polymer Materials of the Russian Academy of Sciences with the support of the Ministry of Science and Higher Education of the Russian Federation, topic no. 0071-2021-0004.

The work was supported by the Russian Science Foundation, project no. 19-13-00340-П.

CONFLICT OF INTEREST

The authors declare no conflict of interest.

REFERENCES

1. S. B. Choi, W. Li, M. Yu, H. Du, J. Fu, and P. X. Do, Smart Mater. Struct. **25**, 043001 (2016).
2. G. Filipcsei, I. Csetneki, A. Szilágyi, and M. Zrínyi, Adv. Polym. Sci. **206**, 137 (2007).
3. Ubaidillah, J. Sutrisno, A. Purwanto, and S. A. Mazlan, Adv. Eng. Mater. **17**, 563 (2015).
4. S. Odenbach, Arch. Appl. Mech. **86**, 269 (2016).

5. M. T. Lopez-Lopez, J. D. G. Durán, L. Yu. Iskakova, and A. Yu. Zubarev, J. Nanofluids **5**, 479 (2016).
6. A. K. Bastola, M. Paudel, L. Li, and W. Li, Smart Mater. Struct. **29**, 123002 (2020).
7. N. Bira, P. Dhagat, and J. R. Davidson, Front. Rob. AI **7**, 588391 (2020).
8. M. Schümann and S. Odenbach, J. Magn. Magn. Mater. **441**, 88 (2017).
9. T. Gundermann and S. Odenbach, Smart. Mater. Struct. **23**, 105013 (2014).
10. G. V. Stepanov, S. S. Abramchuk, D. A. Grishin, L. V. Nikitin, E. Y. Kramarenko, and A. R. Khokhlov, Polymer (Guildf) **48**, 488 (2007).
11. G. V. Stepanov, D. A. Semerenko, A. V. Bakhtiiarov, and P. A. Storozhenko, J. Supercond. Novel Magn. **26**, 1055 (2013).
12. I. A. Belyaeva, E. Y. Kramarenko, and M. Shamonin, Polymer (Guildf) **127**, 119 (2017).
13. S. A. Kostrov, M. Shamonin, G. V. Stepanov, and E. Y. Kramarenko, Int. J. Mol. Sci. **20**, 2230 (2019).
14. D. Isaev, A. Semisalova, Y. Alekhina, L. Makarova, and N. Perov, Int. J. Mol. Sci. **20**, 1457 (2019).
15. G. Glavan, P. Salamon, I. A. Belyaeva, M. Shamonin, and I. Drevenšek-Olenik, J. Appl. Polym. Sci. **135** (18), 46221 (2018).
16. V. V. Sorokin, B. O. Sokolov, G. V. Stepanov, and E. Yu. Kramarenko, J. Magn. Magn. Mater. **459**, 268 (2018).
17. S. A. Kostrov, V. V. Gorodov, B. O. Sokolov, A. M. Muzafarov, and E. Yu. Kramarenko, Polym. Sci., Ser. A **62**, 383 (2020).
18. E. Galipeau and P. Ponte Castañeda, Proc. R. Soc. London, Ser. A **469**, 20130385 (2013).
19. D. V. Saveliev, I. A. Belyaeva, D. V. Chashin, L. Y. Fetisov, D. Romeis, W. Kettl, E. Yu. Kramarenko, M. Saphiannikova, G. V. Stepanov, and M. Shamonin, Materials **13**, 3297 (2020).
20. G. V. Stepanov, E. Y. Kramarenko, and D. A. Semerenko, J. Phys.: Conf. Ser. **412**, 012031 (2013).
21. W. H. Li, Y. Zhou, and T. F. Tian, Rheol. Acta **49**, 733 (2010).
22. A. Stoll, M. Mayer, G. J. Monkman, and M. Shamonin, J. Appl. Polym. Sci. **131**, 131 (2014).
23. M. Cvek, M. Mrlik, J. Sevcik, and M. Sedlacik, Polymers (Basel) **10,** 1411 (2018).
24. R. Moucka, M. Sedlacik, and M. Cvek, Appl. Phys. Lett. **112**, 122901 (2018).
25. T. Tian and M. Nakano, J. Intell. Mater. Syst. Struct. **29**, 151 (2018).
26. M. M. Schmauch, S. R. Mishra, B. A. Evans, O. D. Velev, and J. B. Tracy, ACS Appl. Mater. Interfaces **9**, 11895 (2017).
27. L. Ding, J. Zhang, Q. Shu, S. Liu, S. Xuan, X. Gong, and D. Zhang, ACS Appl. Mater. Interfaces **13**, 13724 (2021).
28. D. Lin, F. Yang, D. Gong, Z. Lin, R. Li, W. Qian, C. Li, S. Jia, and H. Chen, ACS Appl. Mater. Interfaces **13**, 34935 (2021).
29. H. Lu, M. Zhang, Y. Yang, Q. Huang, T. Fukuda, Z. Wang, and Y. Shen, Nat. Commun. **9**, 3944 (2018).
30. M. Farshad and A. Benine, Polym. Test. **23**, 347 (2004).
31. S. A. Kostrov, V. V. Gorodov, A. M. Muzafarov, and E. Yu. Kramarenko, Polym. Sci., Ser. B **64**, 888 (2022).
32. M. A. Khanouki, R. Sedaghati, and M. Hemmatian, Composites, Part B **176**, 107311 (2019).
33. J. Kaleta, M. Królewicz, and D. Lewandowski, Smart Mater. Struct. **20**, 085006 (2011).
34. J. Wu, X. Gong, Y. Fan, and H. Xia, Smart Mater. Struct. **19**, 105007 (2010).
35. S. Chougale, D. Romeis, and M. Saphiannikova, Materials **15**, 645 (2022).
36. J. G. Puente- Córdova, M. E. Reyes-Melo, L. M. Palacios-Pineda, I. A. Martínez-Perales, O. Martínez-Romero, and A. Elías-Zúñiga, Polymers (Basel) **10**, 1343 (2018).
37. G. B. Sohoni and J. E. Mark, J. Appl. Polym. Sci. **34**, 2853 (1987).
38. T. H. Nam, I. Petríková, and B. Marvalová, Polym. Test. **81**, 106272 (2020).
39. E. Coquelle, G. Bossis, D. Szabo, and F. Giulieri, J. Mater. Sci. **41**, 5941 (2006).
40. R. Chokkalingam, R. S. Pandi, and M. Mahendran, J. Compos. Mater. **45**, 1545 (2011).
41. A. Boczkowska, S. F. Awietjan, and R. Wroblewski, Smart Mater. Struct. **16**, 1924 (2007).
42. T. A. Nadzharyan, O. V. Stolbov, Y. L. Raikher, and E. Yu. Kramarenko, Soft Matter **15**, 9507 (2019).
43. G. V. Stepanov, S. I. Kirichenko, E. E. Makhaeva, and E. Yu. Kramarenko, Polym. Sci., Ser. A **65**, 157 (2023).
44. A. Yu. Grossberg and A. R. Khokhlov, *Statistical Physics of Macromolecules* (Nauka, Moscow, 1989; Am. Inst. Phys., New York, 1994).
45. S. Abramchuk, E. Kramarenko, G. Stepanov, L. V. Nikitin, G. Filipcsei, A. R. Khokhlov, and M. Zrínyi, Polym. Adv. Technol. **18**, 883 (2007).
46. A. R. Payne, J. Appl. Polym. Sci. **9**, 3245 (1965).
47. S. Richter, M. Saphiannikova, K. W. Stöckelhuber, and G. Heinrich, Macromol. Symp. **291–292**, 193 (2010).
48. R. Hentschke, Express Polym. Lett. **11**, 278—292 (2017).
49. V. V. Sorokin, E. Ecker, G. V. Stepanov, M. Shamonin, G. J. Monkman, E. Yu. Kramarenko, and A. R. Khokhlov, Soft Matter **10**, 8765 (2014).

Translated by S. Zatonsky

Publisher's Note. Pleiades Publishing remains neutral with regard to jurisdictional claims in published maps and institutional affiliations.